Lattice Realization of Complex Conformal Field Theories: Two-Dimensional Potts Model with $Q > 4$ States

Jesper Lykke Jacobsen[1,2,3] and Kay Jörg Wiese[1]

[1]CNRS-Laboratoire de Physique de l'Ecole Normale Supérieure, PSL Research University, Sorbonne Université, Université Paris Cité, 24 rue Lhomond, 75005 Paris, France

[2]Sorbonne Université, Ecole Normale Supérieure, CNRS, Laboratoire de Physique (LPENS), 75005 Paris, France

[3]Institut de Physique Théorique, CEA, CNRS, Université Paris-Saclay, Orme des Merisiers, Bâtiment 774, 91191 Gif-sur-Yvette, France

(Received 1 March 2024; accepted 6 June 2024; published 16 August 2024)

The two-dimensional Q-state Potts model with real couplings has a first-order transition for $Q > 4$. We study a loop-model realization in which Q is a continuous parameter. This model allows for the collision of a critical and a tricritical fixed point at $Q = 4$, which then emerge as complex conformally invariant theories at $Q > 4$, or even complex Q, for suitable complex coupling constants. All critical exponents can be obtained as analytic continuation of known exact results for $Q \leq 4$. We verify this scenario in detail for $Q = 5$ using transfer-matrix computations.

DOI: 10.1103/PhysRevLett.133.077101

The study of models in two-dimensional statistical mechanics using complex variables goes back to the work of Lee and Yang [1] on the Ising model in a complex magnetic field. Later, complex values of the Ising temperature [2], or the number of states in the Potts model [3] were considered. Here complex analysis is used to draw conclusions about a system for real parameters.

The Q-state Potts model can be reformulated as the Fortuin-Kasteleyn (FK) model [4], in which each lattice bond is erased with a probability related to the temperature. This fragments the lattice into clusters, each with a weight Q which can now take any value. In particular, bond percolation arises for $Q \to 1$. In this formulation, correlation functions relate to probability measures in random geometry (clusters, hulls, backbones, etc), which at the critical temperature form scale and conformally invariant fractals.

In dimension $d = 2$, with Q real and ferromagnetic interactions, criticality occurs for $0 \leq Q \leq Q_c = 4$ [5]; the phase transition turns first order when $Q > 4$, but approximate conformal invariance remains [6]. The same happens in higher dimensions, with $Q_c = 10/3$ for $d \to 6$ [7]. In these examples a stable (critical) fixed point (FP) annihilates with an unstable (tricritical) one upon varying a symmetry-related continuous parameter. This phenomenon, found long ago [8,9], arises in systems as different as deconfined quantum critical points [10] and models of quantum impurity spins coupled to a bath [11].

It has been speculated that in the first-order regime the model may become critical again for complex values of an unknown set of couplings [7,12]. This means that the pair of FPs does not disappear, but moves out in the complex plane for $Q > Q_c$, similar to what happens in the $O(n)$ model for $n > 2$ [13]. In this Letter, we show how this can be achieved in a specific 2D lattice Potts model. Our model contains Q as a free parameter, which can be set to any $Q \in \mathbb{C}$. Our motivation is part of a broader scenario, with ramifications ranging from quantum field theory to probability theory, as we now explain.

A first swathe of exact results about the 2D Potts model was obtained in the 1980s. The lattice models were rewritten in terms of loops (the contours of the FK clusters), which in the continuum limit become level lines of a compactified bosonic field, to which the methods of Coulomb gas (CG) [14] and conformal field theory (CFT) [15] can be applied. Most of these results have since been proved—and in some cases surpassed—by probability theorists, using methods such as Schramm-Loewner evolution (SLE) [16,17] and the conformal loop ensemble (CLE) [18]. Critical exponents (the spectrum) can be derived from CFT [19]. There are indications of a relation to Liouville CFT (LCFT) [20], an exactly solvable interacting CFT with a continuous spectrum, which is unitary for central charge $c \in (1, \infty)$. However, LCFT cannot be the continuum limit of the Potts loop model for generic $Q \in [0, 4]$, since the CG for the latter is known to be nonunitary and has $c \leq 1$ with a discrete spectrum [19].

This situation begs the question whether results for the loop model can be obtained from LCFT by analytic

continuation through complex values of Q. In LCFT the structure constant of three-point correlation functions is given by the so-called DOZZ formula, but analytic continuation of the latter to $c \in (-\infty, 1)$ is impossible. However, a variant of LCFT, called LCFT$_{c\leq 1}$, exists. It has been established [21–23] that the DOZZ-type formula for LCFT$_{c\leq 1}$ [24] correctly predicts three-point functions in the Potts loop model. In contrast, continuation of LCFT$_{c\leq 1}$ and its link with the Potts model for $Q > 4$ has attracted little attention.

The authors of Ref. [12] proposed to analytically continue the relation between Q and the CG coupling constant outside the range $Q \in [0, 4]$. They suggested that a pair of complex CFTs describe the $Q > 4$ model. Our numerical study of the lattice model makes this link precise and reveals that the correspondence extends to a large portion of the complex Q plane. In particular, we provide evidence that the spectra of the two complex CFTs are the appropriate analytic continuation of those [19] for the LCFT$_{c\leq 1}$ loop models. We expect recent results on three- and four-point correlation functions [25–27] and the symmetries of the space of states [28] of the loop models to carry over to the complex CFT as well.

Our starting point is a Q-state Potts model on a triangular lattice with nearest-neighbor interactions K_2, and a three-spin interaction K_3 on each up-pointing triangle. Making an FK expansion [29], one obtains a loop model on a shifted triangular lattice, with five possible diagrams at each vertex. These are, with circles denoting the loci of the Potts spins,

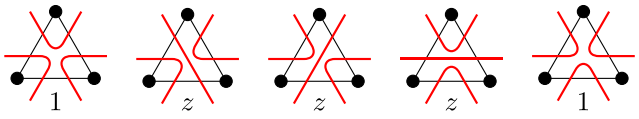

Taking equal weights of the first and last diagram imposes a relation between K_3 and K_2 which ensures self-duality [29]. The three middle diagrams have weight $z = (e^{K_2} - 1)/\sqrt{Q}$. We write this as $z = x + iy$ with $x, y \in \mathbb{R}$. In addition to these local weights, there is a nonlocal factor $n = \sqrt{Q}$ for each red loop. We constrain our study to $\Re e^{K_2} > 0$.

We study this model via the transfer matrix T_L which builds a row of L triangles, with periodic boundary conditions. Thus T_L propagates $\sqrt{3}/2$ lattice spacings upwards and $1/2$ to the right. The operator $\check{R}_k$ that propagates through triangle number k is

$$\check{R}_k = e_{2k-1} + z(e_{2k}e_{2k-1} + 1 + e_{2k-1}e_{2k}) + e_{2k}, \quad (1)$$

where e_i are generators of the periodic Temperley-Lieb algebra [28] on $2L$ sites. Each of the five terms corresponds to one of the above diagrams. We have $T_L = u^{-1}\mathrm{qTr}\check{R}_L \ldots \check{R}_2\check{R}_1$, where qTr denotes the quantum trace over the horizontal space, and u shifts the sites cyclically towards the right. We diagonalize T_L in the space of link patterns, sometimes called standard modules $\mathcal{W}_{j,\rho^2}$, with $2j$ defect lines (FK cluster boundaries) propagating from bottom to top, and (pseudo) momentum ρ describing the winding of lines with respect to the periodic boundary condition; see Ref. [28] for details.

The effective central charge c_L and critical exponents Δ_L are obtained [30] from the finite-L corrections of the leading eigenvalues of T_L. For c_L we need two consecutive sizes, L and $L + 1$. We use the ground-state sector, in which T_L acts on defect-free link patterns ($j = 0$).

For $Q \leq 4$, the model contains a critical and a tricritical point, for fine-tuned values of x. Figure 1 shows c_L as a function of x: c_L is minimal at the critical point ($K_2, K_3 > 0$), and maximal at the tricritical point $K_2 < 0$, $K_3 > 0$. The values at these points agree with the predictions of CFT,

$$Q = 4\cos\left(\frac{\pi}{b}\right)^2, \qquad c(t) = 1 - \frac{6}{t(t-1)}. \quad (2)$$

Here Q defines the parameter b, and we take $t = b > 0$ for the critical point and $t = -b$ for the tricritical one. The corresponding CFTs are denoted B_b. They are minimal models [15] for b rational, but the loop model describes generic values of b (which are real for $Q \leq 4$). We identify B_{-b} with B_{b+1}. Conformal weights are parametrized by the Kac formula

$$h^t_{r,s} = \frac{[t(r-s)+s]^2 - 1}{4(t-1)t}, \quad (3)$$

and below we write $\Delta_{r,s} = 2h^t_{r,s}$ for the corresponding critical exponents.

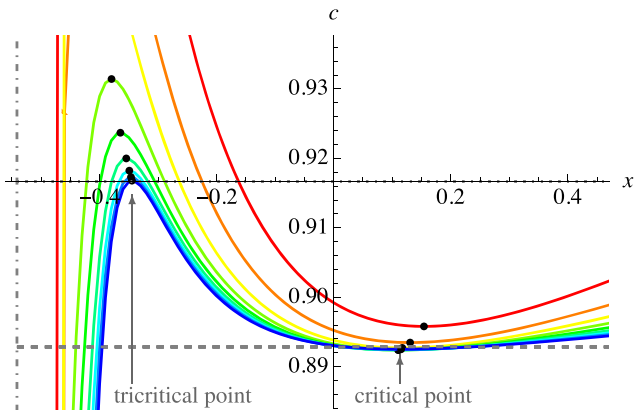

FIG. 1. $c_L(x)$ for $b = 8$, $Q \simeq 3.41421$, using sizes $L = 4$ (red) to 12 (blue). The discontinuity near $x = -1/\sqrt{Q}$ (vertical dot-dashed line) is related to level crossings for $K_2 \to -\infty$. These prevent us from using this approach for smaller Q. CFT predictions are shown for B_8 (dashed line) and $B_{-8} \equiv B_9$ (axis, and gray dots).

Figure 1 shows that upon increasing L, $c_L(z)$ around the critical point becomes shallower, while around the tricritical point it becomes more pointed. The two cases are distinguished by the large-L behavior of the curvature,

$$c_L''(z_c) \sim L^{-2\omega}. \tag{4}$$

$\lim_{L\to\infty} c_L''(z_c) = 0$ defines criticality, $\Re\omega > 0$. ω is related to the dimension Δ of the perturbing operator as

$$\Delta = 2 + \omega^{\text{crit}} \approx 2.57, \qquad \Delta = 2 + \omega^{\text{tricrit}} \approx 1.55 \tag{5}$$

$$\Delta_{3,1}^{\text{crit}} = 18/7 = 2.5714, \qquad \Delta_{3,1}^{\text{tricrit}} = 14/9 = 1.5556. \tag{6}$$

We find good agreement of measurements (5) with the predictions of CFT (6). To summarize: we are able to identify a critical or tricritical point by $c'(z) = 0$, and use a finite-size analysis on $c_L''(z_c)$ to decide whether it is attractive or repulsive. Such a prescription is crucially missing in related work on the O(n) model, where the location of the critical point is known analytically [13].

To proceed, we enlarge our transfer-matrix treatment to complex values of z. The crucial observation is that for all L and Q, $c_L(z)$ is an analytic function of z. It is well represented by a polynomial in z of moderate order (30–100), with a negligible error ($\ll 10^{-4}$). This is valid for $Q \le 4$ and $Q > 4$: a plot for $Q = 5$ is shown in Fig. 2. The critical points are obtained by solving the polynomial equation $c_L'(z) = 0$, which can be done with high precision. The result is shown on the left panel of Fig. 3. There is a pair of critical points next to the imaginary line (in red), and spurious zeros on the boundary of the domain of convergence (in black). The latter roughly indicate the size of the grid of measurement points in Fig. 2. Analytic continuation is so powerful that one can replace the grid by points on the imaginary axis only, see the right panel of Fig. 3. This drastically reduces the work to be done. Extrapolating to $L = \infty$, we find

$$c_{Q=5}^{\text{num}} \approx 1.1377 + 0.0221i, \tag{7}$$

in remarkable agreement with Eq. (2):

$$c_{Q=5}^{\text{CFT}} = 1.13755 + 0.0210687i. \tag{8}$$

This firmly establishes that there is a complex CFT, and that it can be identified from transfer-matrix calculations.

We can go further and obtain the full spectrum of this complex CFT. We study first the spectrum in the ground-state sector, using the quotient representation $\bar{\mathcal{W}}_{0,\mathfrak{q}^2}$ of defect-free link patterns of dimension $[1/(L+1)]\binom{2L}{L}$, where $\sqrt{Q} = \mathfrak{q} + \mathfrak{q}^{-1}$; see [28] for details. Figure 4 shows the exponents corresponding to the first 20 eigenvalues (EVs) in this sector. As the critical points have $x \approx 0$ (see Fig. 3), we take $x = 0$ and plot against $y \ge 0$. The vertical red dashed line indicates the fixed point.

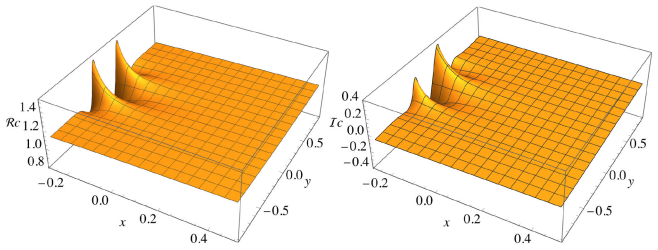

FIG. 2. $Q = 5$, $L = 9$, selected data for $\Re c$ (left) and $\Im c$ right, as a function of $z = x + iy$.

This spectrum contains the spinless primary operators $\Phi_{r,1}$ with eigenvalues $\Delta_{r,1} = 2h_{r,1}^{-b}$, starting with $r = 1$ for the vacuum (baseline). We verify the appearance of $\Phi_{2,1}$ and $\Phi_{3,1}$, with the proper dimensions both for the real and imaginary parts. Descendents have a nonvanishing spin S. The dimension of the primary increases by 1 for each level, and $S/\sqrt{3}$ for the imaginary part. The latter arises since T_L propagates by $\sqrt{3/4}$ upwards, and $1/2$ rightwards, with ratio $\sqrt{3}$. Using $L_{-N,-\bar{N}}\Phi_{r,1}$ as a shorthand for any descendent on chiral level N and antichiral level $\bar{N}$, we get

$$\Delta(L_{-N,-\bar{N}}\Phi_{r,1}) = \Delta_{r,1} + (N + \bar{N}) + \frac{1}{\sqrt{3}}(N - \bar{N})i. \tag{9}$$

The $\Phi_{r,1}$ form Kac modules with one null state on level r. The content of primaries and the structure of the modules were predicted for $Q < 4$ [19] and numerically verified for a corresponding loop model [32]. We see in Fig. 4 that all of this is perfectly respected at $Q = 5$ for the 20 lowest-lying states: we conjecture that the results for the spectrum carry over to the complex CFT by analytic continuation. Generalizations to sectors with defect lines will be discussed elsewhere [31].

From finite-size scaling we find ω, which satisfies $2 + \omega \approx \Delta_{3,1} = 2h_{3,1}^{-b}$,

$$\omega = -0.12(2) + 0.62(2)i, \qquad \Delta_{3,1} = 1.9083 + 0.598652i.$$

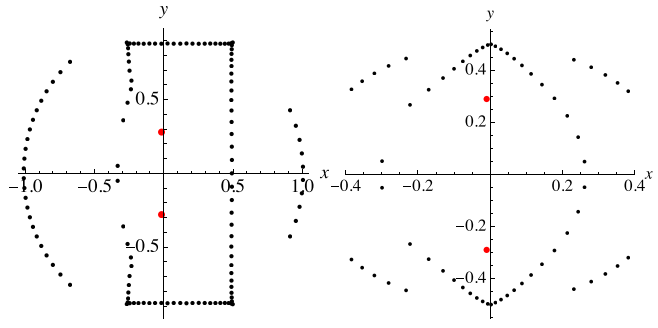

FIG. 3. Zeros of $c'(z)$. Left: $L = 10$ using measures on a rectangular grid of points. Right: $L = 13$ using measures only on the imaginary axis.

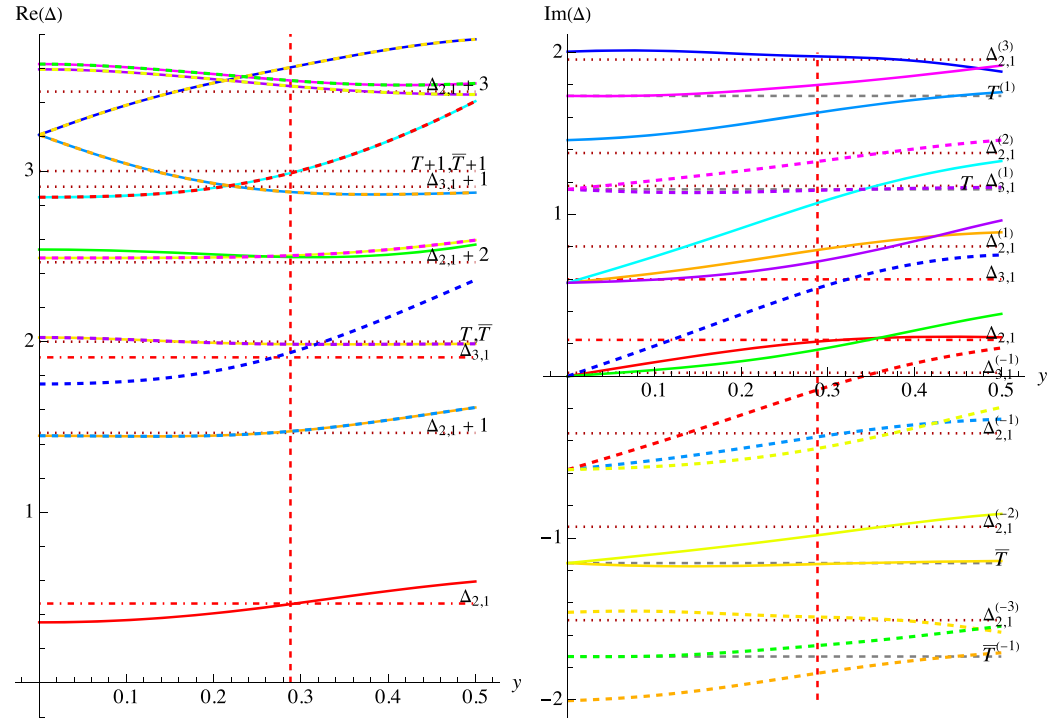

state	operator	spin
1	GS $= \Phi_{1,1}$	0
2	$\epsilon = \Phi_{2,1}$	0
3	$L_{0,-1}\Phi_{2,1}$	−1
4	$L_{-1,0}\Phi_{2,1}$	1
5	$\epsilon' = \Phi_{3,1}$	0
6	$\overline{T} \equiv L_{0,-2}\Phi_{1,1}$	−2
7	$T \equiv L_{-2,0}\Phi_{1,1}$	2
8	$L_{0,-2}\Phi_{2,1}$	−2
9	$L_{-2,0}\Phi_{2,1}$	2
10	$L_{-1,-1}\Phi_{2,1}$	0
11	$L_{0,-1}\Phi_{3,1}$	−1
12	$L_{-1,0}\Phi_{3,1}$	1
13	$L_{0,-1}\overline{T}$	−3
14	$L_{-1}T$	3
15	$L_{0,-3}\Phi_{2,1}$	−3
16	$L_{-3,0}\Phi_{2,1}$	3
17	$L_{-1,-2}\Phi_{2,1}$	−1
18	$L_{-2,-1}\Phi_{2,1}$	1
19	$L_{0,-3}\Phi_{2,1}$	−3
20	$L_{-3,0}\Phi_{2,1}$	3

FIG. 4. Real and imaginary part $\Delta^{(S)}_{r,s}$ of spectrum in the ground-state sector for $Q = 5$, $L = 14$, taking only the first 20 EVs. Primaries in red, dashed lines; descendents in darker red, dotted lines. The red dashed vertical lines denote the position of the critical point. For details, see Ref. [31].

We now proceed to complex values of Q. In Fig. 5 we show the location of the zeros of $c'_L(z)$ evaluated in the plane for $Q = 5 + 2i$ and $Q = 8 + i$. Since $Q^* \neq Q$ they are no longer complex conjugate of each other, and the two fixed points are distinct. We can again measure the central charge and compare to the theoretical prediction, first for $Q = 5 + 2i$,

$$c^{\text{num}}_{\text{upper}} \approx 1.108 + 0.252i, \qquad c^{\text{num}}_{\text{lower}} \approx 1.247 + 0.228i,$$
$$c(-b_Q) = 1.1122 + 0.2505i, \qquad c(b_Q) = 1.2464 + 0.2293i.$$

For $Q = 8 + i$ we find

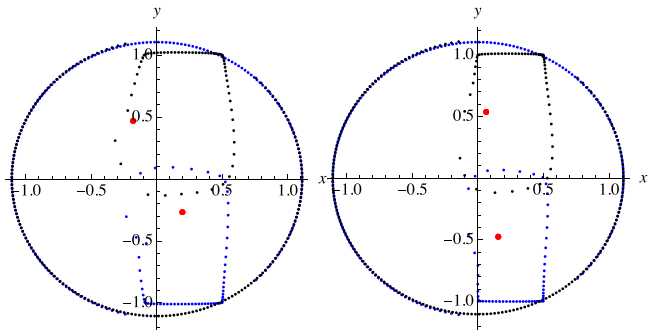

FIG. 5. Zeros of $c'(z)$ at $L = 9$. Left: $Q = 5 + 2i$. Right: $Q = 8 + i$. We have used separate fits for the upper (black) and lower (blue) half planes.

$$c^{\text{num}}_{\text{upper}} \approx 1.407 + 0.207i, \qquad c^{\text{num}}_{\text{lower}} \approx 1.479 - 0.047i,$$
$$c(-b_Q) = 1.4073 + 0.2041i, \qquad c(b_Q) = 1.4778 - 0.0420i.$$

Both cases are in good agreement. Our procedure continues to work for $Q = 10$, $Q = 20$, and $Q = 40$.

We have shown that according to definition (4), for $Q < 4$ and $Q = 5 + 2i$, both a critical and a tricritical point exist, while for $Q = 5$ and $Q = 8 + i$ both points are tricritical. In general, criticality means $\Re\Delta_{3,1} > 2$. Inside the yellow-shaded region in Fig. 6, one point is critical and one tricritical, whereas outside both are tricritical. The boundary is given by

$$Q(\phi) = 2 + 2\cos\left(\frac{2\pi}{1 + i\phi}\right), \qquad \phi \in \mathbb{R}. \tag{10}$$

Finally we draw the two critical points for complex Q, with $\Re Q > 4$, as well as their complex conjugates, which are critical points for Q^*. Moving Q to the real axis, the four points merge in pairs, and only two fixed points remain.

Our model can be reformulated as non-Hermitian quantum mechanics. To this end, we take an anisotropic limit of the transfer matrix, to find a Hamiltonian [33]

$$\mathcal{H} = \sum_{i=1}^{L} e_i + \tilde{z}(e_i e_{i+1} + e_{i+1} e_i). \tag{11}$$

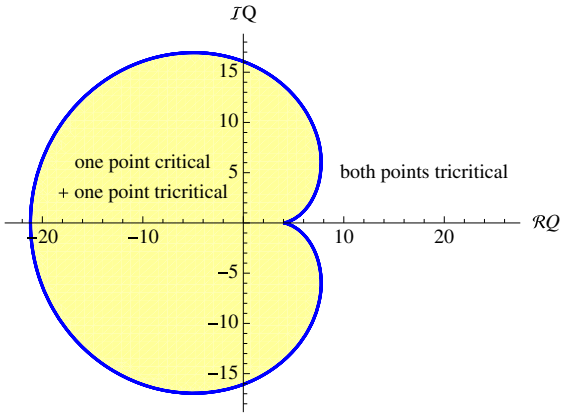

FIG. 6. In yellow, the region where $\Re\Delta_{3,1}(b) > 2$. In blue, the parametric curve (10).

For real $Q \in [Q^*, 4)$ with $Q^* \simeq 2.25$, a critical phase terminated by a tricritical end point is found. We posit that for $Q > 4$ and $Q \in \mathbb{C}$, the spin chain exhibits the same complex critical points studied above [31]. For integer Q, the results should equal those for the quantum chain formulated in terms of Potts spins, but details (such as multiplicities and operator product expansions) may differ due to the change of representation.

We conclude by remarks on related work. First, a classification of critical points with S_Q symmetry was made in [34]. The case $e^{K_2} < 0$, excluded here, may be relevant [31,35] for the nonferromagnetic solutions with $Q > 4$ studied there. Second, [13] studied complex CFT in the $O(n)$ model. Because of the different global symmetry [28] the $O(n)$ CFT differs from the Potts CFT studied here. In particular, it contains $\Phi_{r,1}$ only for $r \in 1 + 2\mathbb{N}$, and has a different phase diagram.

Acknowledgments—We thank Y.-C. He, A. Ludwig, A. Nahum, S. Ribault, S. Rychkov, and H. Saleur for stimulating discussions. This work was supported by the French Agence Nationale de la Recherche (ANR) under Grant No. ANR-21-CE40-0003 (project CONFICA), and in part by Grant No. NSF PHY-2309135 to the KITP.

[1] T. D. Lee and C. N. Yang, Statistical theory of equations of state and phase transitions, II. Lattice gas and Ising model, Phys. Rev. **87**, 410 (1952).
[2] M. E. Fisher, The nature of critical points, in *Lecture Notes in Theoretical Physics*, edited by W. E. Brittin, Volume 7c (University of Colorado Press, Denver, Colorado, 1965), pp. 1–159.
[3] J. Salas and A. D. Sokal, Transfer matrices and partition-function zeros for antiferromagnetic Potts models. I. General theory and square-lattice chromatic polynomial, J. Stat. Phys. **104**, 609 (2001).
[4] C. M. Fortuin and P. W. Kasteleyn, On the random-cluster model: I. Introduction and relation to other models, Physica (Amsterdam) **57**, 536 (1972).
[5] R. J. Baxter, Potts model at the critical temperature, J. Phys. C **6**, L445 (1973).
[6] H. Ma and Y.-C. He, Shadow of complex fixed point: Approximate conformality of $Q > 4$ Potts model, Phys. Rev. B **99**, 195130 (2019).
[7] K. J. Wiese and J. L. Jacobsen, The two upper critical dimensions of the Ising and Potts models, J. High Energy Phys. 05 (2024) 092.
[8] J. L. Cardy, M. Nauenberg, and D. J. Scalapino, Scaling theory of the Potts-model multicritical point, Phys. Rev. B **22**, 2560 (1980).
[9] G. Delfino and J. Cardy, The field theory of the $Q \to 4^+$ Potts model, Phys. Lett. B **483**, 303 (2000).
[10] C. Wang, A. Nahum, M. A. Metlitski, C. Xu, and T. Senthil, Deconfined quantum critical points: Symmetries and dualities, Phys. Rev. X **7**, 031051 (2017).
[11] A. Nahum, Fixed point annihilation for a spin in a fluctuating field, Phys. Rev. B **106**, L081109 (2022).
[12] V. Gorbenko, S. Rychkov, and B. Zan, Walking, weak first-order transitions, and complex CFTs II, two-dimensional Potts model at $Q > 4$, SciPost Phys. **5**, 50 (2018).
[13] A. Haldar, O. Tavakol, H. Ma, and T. Scaffidi, Hidden critical points in the two-dimensional $O(n > 2)$ model: Exact numerical study of a complex conformal field theory, Phys. Rev. Lett. **131**, 131601 (2023).
[14] B. Nienhuis, Critical behaviour of two-dimensional spin models and charge asymmetry in the Coulomb gas, J. Stat. Phys. **34**, 731 (1984).
[15] A. A. Belavin, A. M. Polyakov, and A. B. Zamolodchikov, Infinite conformal symmetry in two-dimensional quantum field theory, Nucl. Phys. **B241**, 333 (1984).
[16] J. Cardy, SLE for theoretical physicists, Ann. Phys. (N.Y.) **318**, 81 (2005).
[17] G. F. Lawler, Schramm-Loewner evolution, arXiv: 0712.3256.
[18] S. Sheffield, Exploration trees and conformal loop ensembles, Duke Math. J. **147**, 79 (2009).
[19] P. Di Francesco, H. Saleur, and J. B. Zuber, Relations between the Coulomb gas picture and conformal invariance of two-dimensional critical models, J. Stat. Phys. **49**, 57 (1987).
[20] J. Kondev, Liouville field theory of fluctuating loops, Phys. Rev. Lett. **78**, 4320 (1997).
[21] G. Delfino and J. Viti, On three-point connectivity in two-dimensional percolation, J. Phys. A **44**, 032001 (2010).
[22] M. Picco, R. Santachiara, J. Viti, and G. Delfino, Connectivities of Potts Fortuin-Kasteleyn clusters and time-like Liouville correlator, Nucl. Phys. **B875**, 719 (2013).
[23] Y. Ikhlef, J. L. Jacobsen, and H. Saleur, Three-point functions in $c \leq 1$ Liouville theory and conformal loop ensembles, Phys. Rev. Lett. **116**, 130601 (2016).
[24] A. B. Zamolodchikov, Three-point function in the minimal Liouville gravity, Theor. Math. Phys. **142**, 183 (2005).
[25] Y. He, J. L. Jacobsen, and H. Saleur, Geometrical four-point functions in the two-dimensional critical Q-state Potts model: The interchiral conformal bootstrap, J. High Energy Phys. 12 (2020) 019.

[26] L. Grans-Samuelsson, J. L. Jacobsen, R. Nivesvivat, S. Ribault, and H. Saleur, From combinatorial maps to correlation functions in loop models, SciPost Phys. **15**, 147 (2023).
[27] R. Nivesvivat, S. Ribault, and J. L. Jacobsen, Critical loop models are exactly solvable, arXiv:2311.17558 [SciPost Phys. (to be published)].
[28] J. L. Jacobsen, S. Ribault, and H. Saleur, Spaces of states of the two-dimensional $O(n)$ and Potts models, SciPost Phys. **14**, 092 (2023).
[29] F. Y. Wu and K. Y. Lin, On the triangular Potts model with two- and three-site interactions, J. Phys. A **13**, 629 (1980).
[30] H. W. J. Blöte, J. L. Cardy, and M. P. Nightingale, Conformal invariance, the central charge, and universal finite size amplitudes at criticality, Phys. Rev. Lett. **56**, 742 (1986).
[31] J. L. Jacobsen and K. J. Wiese (to be published).
[32] J. L. Jacobsen and H. Saleur, Bootstrap approach to geometrical four-point functions in the two-dimensional critical Q-state Potts model: A study of the s-channel spectra, J. High Energy Phys. 01 (2019) 084.
[33] Y. Ikhlef, J. L. Jacobsen, and H. Saleur, A Temperley–Lieb quantum chain with two- and three-site interactions, J. Phys. A **42**, 292002 (2009).
[34] G. Delfino and E. Tartaglia, Classifying Potts critical lines, Phys. Rev. E **96**, 042137 (2017).
[35] R. J. Baxter, Critical antiferromagnetic square-lattice Potts model, Proc. R. Soc. A **383**, 43 (1982).